11-2015

Unoccupied electronic structure of Ni2MnGa ferromagnetic shape memory alloy

M. Maniraj
UGC-DAE Consortium for Scientific Research

S. W. D'Souza
UGC-DAE Consortium for Scientific Research

Abhishek Rai
UGC-DAE Consortium for Scientific Research

Deborah L. Schlagel
Ames Laboratory, schlagel@ameslab.gov

Thomas A. Lograsso
Iowa State University and Ames Laboratory, lograsso@ameslab.gov

See next page for additional authors

Unoccupied electronic structure of Ni2MnGa ferromagnetic shape memory alloy

Abstract
Momentum resolved inverse photoemission spectroscopy measurements show that the dispersion of the unoccupied bands of Ni2MnGa is significant in the austenite phase. In the martensite phase, it is markedly reduced, which is possibly related to the structural transition to an incommensurate modulated state in the martensite phase. Based on the first principle calculations of the electronic structure of Ni–Mn–Ga, we show that the modification of the spectral shape with surface composition is related to change in the hybridization between the Mn 3*d* and Ni 3*d*-like states that dominate the unoccupied conduction band.

Keywords
A. Ferromagnetic shape memory alloy, D. Martensite transition, E. Inverse photoemission spectroscopy, E. Korriga–Kohn–Rostoker method

Disciplines
Atomic, Molecular and Optical Physics | Materials Science and Engineering | Metallurgy | Semiconductor and Optical Materials

Comments
This is a manuscript of the article published as Maniraj, M., Abhishek Rai, D. L. Schlagel, T. A. Lograsso, Aparna Chakrabarti, and S. R. Barman. "Unoccupied electronic structure of Ni 2 MnGa ferromagnetic shape memory alloy." *Solid State Communications* 222 (2015): 1-4. DOI: 10.1016/j.ssc.2015.08.003. Posted with permission.

Authors
M. Maniraj, S. W. D'Souza, Abhishek Rai, Deborah L. Schlagel, Thomas A. Lograsso, Aparna Chakrabarti, and S. R. Barman

Unoccupied electronic structure of Ni_2MnGa ferromagnetic shape memory alloy

M. Maniraj[a,*], S. W. D'Souza[a], Abhishek Rai[a], D. L. Schlagel[b], T. A. Lograsso[b,c], Aparna Chakrabarti[d], S. R. Barman[a]

[a] *UGC-DAE Consortium for Scientific Research, Khandwa Road, Indore, 452001, Madhya Pradesh, India*
[b] *Division of Materials Sciences and Engineering, Ames Laboratory, Ames, Iowa 50011, USA*
[c] *Department of Materials Science and Engineering, Iowa State University, Ames, Iowa 50011, USA*
[d] *Raja Ramanna Centre for Advanced Technology, Indore 452013, Madhya Pradesh, India*

Abstract

Momentum resolved inverse photoemission spectroscopy measurements show that the dispersion of the unoccupied bands of Ni_2MnGa is significant in the austenite phase. In the martensite phase, it is markedly reduced, which is possibly related to the structural transition to an incommensurate modulated state in the martensite phase. Based on first principle calculations of the electronic structure of Ni-Mn-Ga, we show that the modification of the spectral shape with surface composition is related to change in the hybridization between the Mn 3*d* and Ni 3*d*-like states that dominate the unoccupied conduction band.

Keywords: , E. Inverse photoemission spectroscopy, E. Korriga-Kohn-Rostoker method, A. Ferromagnetic shape memory alloy, D. Martensite transition

1. Introduction

The magnetic shape memory alloys (MSMA) have been a topic of active research in recent years from the point of view of both basic science as well as applied research.[1, 2, 3, 4, 5, 6, 7, 8] Among the different MSMA materials, Ni_2MnGa is most important due to its multifunctional properties such as large magnetic field induced strain of up to 10% at about 1 T applied magnetic field, large negative magnetoresistance and magnetocaloric properties.[3, 6, 7, 9] The electronic structure of Ni_2MnGa has been extensively studied by photoemission spectroscopy and density functional theory to understand the origin of martensite phase transition.[10, 11, 12, 13, 14, 15, 16, 17]

At room temperature (RT), Ni_2MnGa is ferromagnetic and exists in the austenite state. The martensite transition and Curie temperatures of Ni_2MnGa are 206 K and 376 K, respectively.[18] In the austenite phase, Ni_2MnGa has cubic $L2_1$ crystal structure with lattice constant of 5.825 Å.[19] The cubic $L2_1$ structure of Ni_2MnGa can be visualized (Fig. 1) as a face-centered-cubic lattice with a basis of four atoms Ga, Ni, Mn and Ni placed along the diagonal at (0, 0, 0), (0.25, 0.25, 0.25), (0.5, 0.5, 0.5) and (0.75, 0.75, 0.75), respectively. Angle-dependent x-ray photoemission spectroscopy study shows that Ni_2MnGa(100) surface is Mn−Ga terminated.[20] Low energy electron diffraction (LEED) and scanning tunnelling microscopy measurements revealed that the Ni_2MnGa surface has bulk termination.[20, 21] In the martensite phase, Ni_2MnGa exhibits a modulated structure that can be described as a shuffling of the (010) planes along [100] direction of the tetragonal primitive cell of the austenite phase *i.e.* along [110] direction of the $L2_1$ structure.[22, 23, 24] The modulation is sevenfold (7M) and is driven by transverse acoustic TA_2 soft-phonon mode along [110] direction of the $L2_1$ structure.[25] Although the modulation wave vector was earlier reported to be commensurate,[22] recent studies have shown that it is incommensurate both in bulk[24, 25] as well as at the surface[26].

On the theoretical front, Fujii *et al.* have studied the electronic structure of Ni_2MnGa using Korringa Kohn Rostoker (KKR) method.[10] They found that the states around the Fermi level (E_F) exhibit band Jahn-Teller effect that possibly stabilizes the martensite phase. Recently, Kumura *et al.*[17] reported that Ni-Mn-Ga, which has a high valence electron concentration, undergoes martensite phase transition due to large density of states (DOS) in Ni 3*d* e_g states near E_F. Barman *et al.*[13] have studied the equilibrium structure and electronic properties of Ni_2MnGa for both the martensite and austenite phases. They found a splitting of minority spin Ni 3*d*-like states below E_F.

The x-ray absorption near-edge structure studies conducted by Sathe *et al.*[27] for several Ni-Mn-Ga samples revealed interesting changes in the partial DOS (PDOS) of Mn atom. Strong variation in the unoccupied PDOS of Mn has been observed at the austenite to martensite phase transition. Ultraviolet pho-

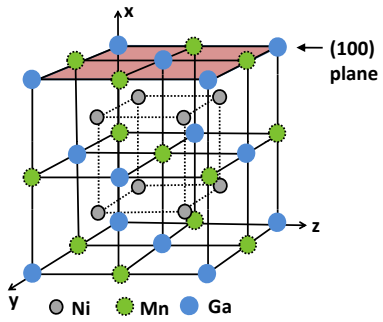

Figure 1: The $L2_1$ unit cell of Ni_2MnGa in the austenite phase.

*Corresponding author
Email address: mr.maniraj@gmail.com (M. Maniraj)

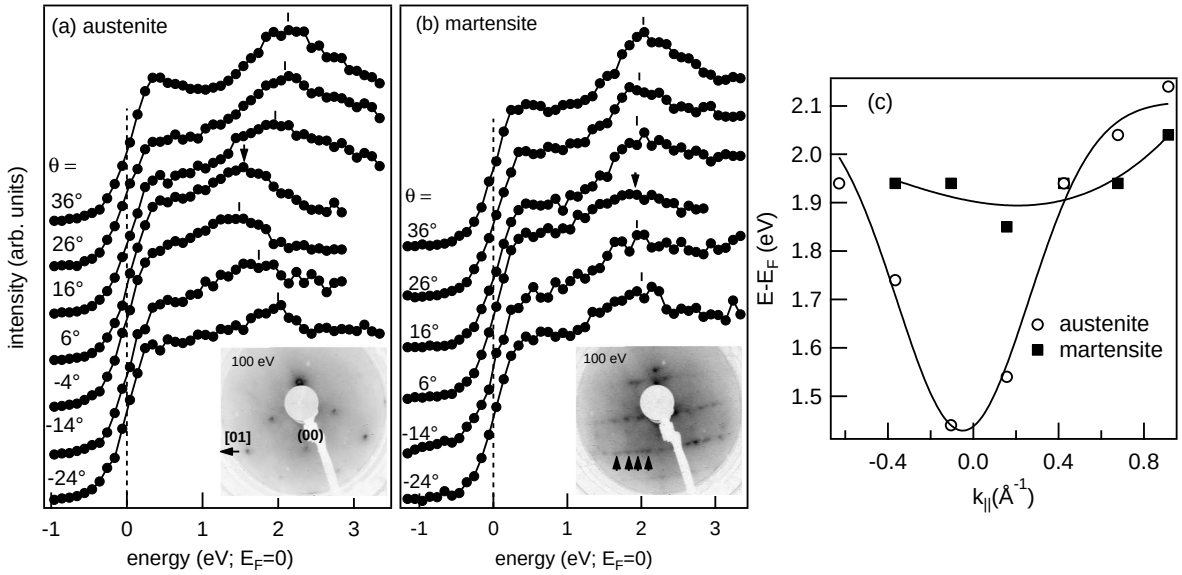

Figure 2: (a) KRIPES spectra of $Ni_2MnGa(100)$ measured in the austenite phase at room temperature along [01] direction, as shown in the inset. Inset shows the LEED pattern recorded in the austenite phase in inverted gray scale, where black indicates highest brightness. (b) KRIPES spectra measured in the martensite phase at 100 K along same direction. Inset shows LEED pattern recorded in the martensite phase at 100 K. Some of the satellite spots are indicated by arrows. (c) E($k_{||}$) dispersion of the peaks shown by ticks in (a) and (b). The continuous line serves as a guide to the eye.

toemission study of $Ni_2MnGa(100)$ across the martensite phase transition shows a large spectral weight redistribution near E_F, which established existence of a pseudogap around E_F.[15] The pseudogap arises due to charge density wave that is associated with an incommensurate periodic lattice distortion.[15] Thus, the martensite transition is closely related to the modification of electronic states below and above E_F. Hence, the behavior of the unoccupied states near E_F in Ni-Mn-Ga across the martensite transition, are expected to play an important role, but such studies do not exist in literature. In the present work, we report the unoccupied electronic structure of Ni-Mn-Ga as a function of surface composition and changes in the unoccupied electronic band structure of $Ni_2MnGa(100)$ between austenite and martensite phases using momentum (k) resolved inverse photoemission spectroscopy (KRIPES).

2. Experimental Method

$Ni_2MnGa(100)$ crystal was grown by Bridgman method.[28] The crystal was cut along [100] axis in the austenite phase and then mechanically and chemically polished. The KRIPES measurements were performed in a μ metal chamber at a base pressure of 5×10^{-11} mbar. The measurements were performed in the isochromat mode. The spectrometer comprises of a variable energy Stoffel-Johnson design electron source and a CaF_2/acetone photon detector.[29] The total energy resolution is about 0.5 eV. The electron beam divergence is 5°, which gives a momentum resolution of nearly 0.13 $Å^{-1}$.[30] The electron beam current variation has been accounted for by normalizing the measured counts by the sample current.[31] Angle between the electron gun and photon detector was kept fixed at 45°. For the k resolved mesurements, the sample was rotated along the polar angle to change the angle of incidence (θ) of the electron beam. Positive θ refers to rotation of perpendicular axis of the sample towards the detector.

An atomically clean and stoichiometric Ni_2MnGa surface was obtained by Ar ion sputtering with 1.5 keV energy for 15−30 min followed by resistive heating for 1 h.[20, 26] Annealing the crystal at 830 K restores the stoichiometric surface composition of $Ni_{1.95}Mn_{0.89}Ga_{1.16}$ (Mn:Ni= 0.46). Since the transition temperatures are highly sensitive to composition,[18, 32] the stoichiometric surface was confirmed by the similarity of the surface martensite transition start temperature (201 K, determined by LEED) to the bulk martensite transition temperature.[26, 15] $Ni_2MnGa(100)$ surfaces with different compositions have been obtained by varying the Mn:Ni ratio that sensitively depends on the annealing temperature.[20, 26]

The electronic structure calculations were carried out by using fully relativistic spin polarized Korringa Kohn Rostoker method.[33] The details of calculations can be found in [34]. In order to compare the experimental IPES spectrum with theory, the DOS was multiplied with the Fermi function and then convoluted with a Voigt function. In the Voigt function, full width at half maximum (FWHM) of the Gaussian component represents the instrumental resolution. The FWHM of energy dependent Lorentzian that represents the life-time broadening was taken as $0.3E$, where E is the energy with respect to E_F.[35] Following Ref. [36], the inelastic background and matrix elements were not considered in calculation of the IPES spectra.

3. Results and Discussion

Figure 2(a) show KRIPES spectra of $Ni_2MnGa(100)$ measured in the austenite phase. The spectra have been measured

along [01] direction (inset in Fig. 2(a)), as defined in Ref.[26]. The LEED pattern recorded at room temperature shows four fold symmetry, characteristic of (100) surface termination of the bulk $L2_1$ structure.[20, 26] At $\theta = 6°$, a peak is observed at about 1.5 eV (arrow in Fig. 2(a)). With increasing θ, this peak exhibits significant dispersion towards higher energy with momentum parallel to surface ($\mathbf{k}_{\|}$). The E($\mathbf{k}_{\|}$) plot corresponding to this peak is shown in Fig. 2(c) (open circles). From the band structure calculations as discussed below, these bands are dominated by Mn 3*d* states.

We now turn to the martensite phase KRIPES data of Ni_2MnGa measured at 100 K. In the martensite phase, Ni_2MnGa has twinned crystal structure. The presence of multiple twins can significantly smear out the direct momentum conserved electronic transitions and can lead to a situation similar to a measurement on polycrystalline sample. Therefore, to achieve the single variant phase (i.e. maintaining the single crystallinity and yet with modulated crystal structure), we applied an uniaxial pressure on the sample along [11] direction of the austenite body-centered tetragonal unit cell.[26, 15] The LEED pattern of uniaxially stressed sample exhibits modulation below the surface martensite start temperature (201 K). The presence of satellite spots only along [10] direction of $L2_1$ austenite structure confirms the existence of modulation and sample is in the single variant phase (inset in Fig. 2(b)). Bulk modulation in Ni_2MnGa is associated with a shuffle of the (010) planes along [100] direction of the tetragonal primitive cell of the austenite phase *i.e.* along [110] direction of the $L2_1$ structure. So, at the bulk truncated (100) surface, modulation takes place along [01] direction of the austenite phase. In Ref. [26], we have analyzed the spot separation and found that nature of modulation is incommensurate 7M for stoichiometric Ni_2MnGa.[25] Direct comparison of the LEED pattern (inset in Figs. 2 (a) and (b)) reveals that modulation appears along [01] direction of the austenite phase and hence Brillouin zone size in the martensite phase is reduced by a factor of 7 along this direction compared to that of the austenite phase. This new Brillouin zone size (~0.15 $Å^{-1}$) is comparable to our spectrometer momentum resolution.

At θ= 6°, a broad peak appears at around 1.9 eV above E_F (arrow in Fig. 2(b)). This peak primarily arises from Mn 3*d* states as in the case of austenite phase.[13] It shows a weak dispersion with increasing θ along [01] direction. E($\mathbf{k}_{\|}$) plot for this peak is shown in Fig. 2(c) (filled squares), which shows that the dispersion in martensite phase is weaker than the austenite phase. Thus, our KRIPES data reveal significant difference in the nature of dispersion of the surface band related to Mn 3*d* states in the martensite phase. This is related to the structural change brought about by modulation.

A set of spectra measured at room temperature for different surface composition of Ni-Mn-Ga is shown in Fig. 3(a). The sputter-annealed surface with Mn:Ni = 0.3 shows a broad feature around 2.1 eV and it becomes stronger at Mn:Ni = 0.46. Between Mn:Ni ratio of 0.3 to 0.5, the peak position shifts towards E_F from 2.1 to 1.5 eV (ticks in Fig. 3(a)).

In order to gain insight about the electronic origin of the experimentally observed spectral shape and the shift in the peak position, we have compared the experimental spectra with the electronic structure calculations in Fig. 3(b) and (c). It may be noted that the calculated spectra is based on the total DOS, which is an integration of the dispersion curves over the whole Brillouin zone. On the other hand, the experimental spectra are momentum resolved and thus equivalent to DOS that is integrated over a part of the Brillouin zone. Nevertheless, this comparison is partially valid because nonstoichiometry and the resulting disorder present at the surface would enhance surface mediated indirect transitions,[15, 37] and indeed the spectral shape somewhat similar to IPES spectra of polycrystalline Ni_2MnGa.[32] Fig. 3(b) shows the calculated total DOS, and a shift in the peak position is readily visible. The calculated con-

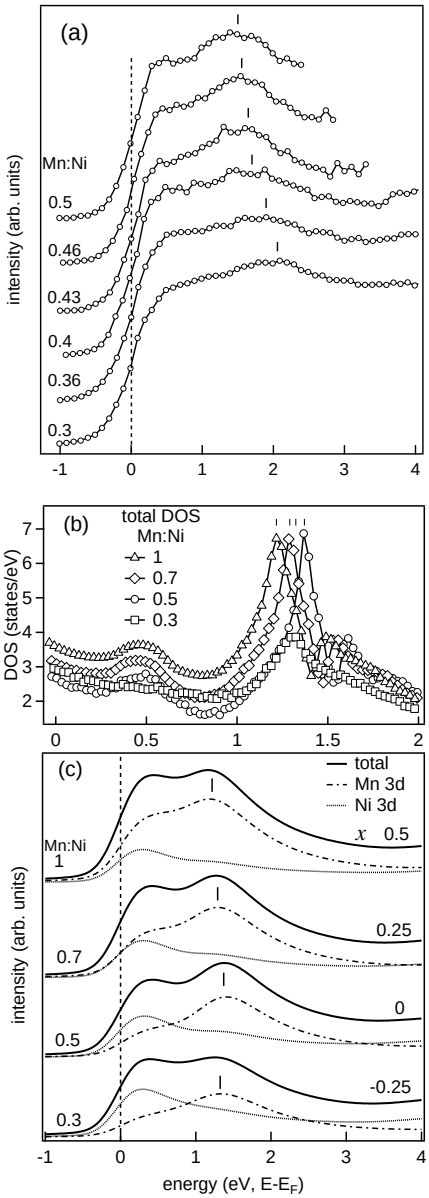

Figure 3: (a) Inverse photoemission spectra measured at θ= 6° for different surface compositions of Ni-Mn-Ga, as indicated by the Mn:Ni ratio. All the spectra are measured at RT and normalized to the same height. (b) The calculated total DOS and (c) convoluted total DOS, Mn 3*d* and Ni 3*d* PDOS of $Ni_{2-x}Mn_{1+x}Ga$ in the cubic austenite phase.

duction band spectra shows two peaks for all the compositions (Fig. 3(c)). **It may be noted that when compared to the total DOS shown in Fig. 3(b), the shift of the peak position is less evident in Fig. 3(c) because of the broadening due to instrumental resolution of 0.5 eV.** Ni 3*d* PDOS shows a peak around 0.4 eV, while Mn 3*d* PDOS also shows a peak at similar energy and its intensity increases with increasing Mn:Ni ratio. On the other hand, a dominant peak is observed at higher energy that arises entirely from Mn 3*d* states, for example at 1.4 eV for Mn:Ni= 0.5, at 1.3 eV for Mn:Ni = 0.7, and at 1.2 eV for Mn:Ni = 1 (see ticks in Fig. 3(c)). Thus, clearly, this peak shows a systematic shift towards E_F with increasing Mn:Ni ratio as the Mn 3*d*−Mn 3*d* hybridization dominates over Mn 3*d*−Ni 3*d* hybridization.

4. Conclusion

In the present work, we have investigated the unoccupied electronic structure of $Ni_2MnGa(100)$ using KRIPES. We find a significant difference in the KRIPES spectra of $Ni_2MnGa(100)$ performed along [01] direction of the $L2_1$ structure: a transition from a substantial energy dispersion of state in the austenite phase to state with weak dispersion in the martensite phase. Origin for weak dispersion in the martensite phase is attributed to their modulated structure *i.e.* the increased unit cell dimension due to modulation that reduces the dimension of the Brillouin zone size so much that it becomes comparable to the experimental angular resolution. Spectra measured as a function of surface composition from Ni-excess to stoichiometric Ni-Mn-Ga show that peak energy position is sensitive to the composition. The calculated total DOS as a function of composition indicates that the peak energy position shift is due to the influence of Mn 3*d*−Ni 3*d* hybridization.

Acknowledgment

S. Singh and J. Nayak are thanked for useful discussions and support during the experiment. This work has been performed using the inverse photoemission spectroscopy workstation fabricated under the Department of Science and Technology Project SP/S2/M-06/99. M.M. and S.W.D. are thankful to Council of Scientific and Industrial Research, India for research fellowship.

References

[1] L. Mañosa, D. Gonzalez-Alonso, E. Bonnot, M. Barrio, J. Tamarit, S. Aksoy, M. Acet Nature. Mater. **9** (2010) 478.
[2] I. Takeuchi, O.O. Famodu, J.C. Read, M.A. Aronova, K.-S. Chang, C. Craciunescu, S.E. Lofland, M. Wuttig, F.C. Wellstood, L. Knauss, A. Orozco, Nature Mater. **2** (2003) 180.
[3] A. Sozinov, A.A. Likhachev, N. Lanska, K. Ullakko, Appl. Phys. Lett. **80** (2002)1746.
[4] T. Krenke, E. Duman, M. Acet, E.F. Wassermann, X. Moya, L. Mañosa, A. Planes, Nature Mater. **4** (2005) 450.
[5] R. Kainuma, Y. Imano, W. Ito, Y. Sutou, H. Morito, S. Okamoto, O. Kitakami, K. Oikawa, A. Fujita, T. Kanomata, K. Ishida, Nature **439** (2006) 957.
[6] K. Ullakko, J.K. Huang, C. Kantner, R.C.O. Handley, V.V. Kokorin, Appl. Phys. Lett. **69** (1996) 1966.
[7] C. Biswas, R. Rawat, S.R. Barman, Appl. Phys. Lett. **86** (2005) 202508; S. Singh, R. Rawat, S.R. Barman, Appl. Phys. Lett. **99** (2011) 021902.
[8] S. Singh, R. Rawat, S.E. Muthu, S.W. D'Souza, E. Suard, A. Senyshyn, S. Banik, P. Rajput, S. Bhardwaj, A.M. Awasthi, R. Ranjan, S. Arumugam, D.L. Schlagel, T.A. Lograsso, A. Chakrabarti, S.R. Barman, Phys. Rev. Lett. **109** (2012) 246601.
[9] J. Marcos, L. Mañosa, A. Planes, F. Casanova, X. Batlle, A. Labarta, Phys. Rev. B **68** (2003) 09440.
[10] S. Fujii, S. Ishida, S. Asano, J. Phys. Soc. Japan **58** (1989) 3657.
[11] A. Ayuela, J. Enkovaara, R.M. Nieminen, J. Phys.: Condens. Matter **14**, 5325 (2002).
[12] C. Bungaro, K.M. Rabe, A. Dal Corso, Phys. Rev. B **68** (2003) 134104.
[13] S.R. Barman, S. Banik, A. Chakrabarti Phys. Rev. B **72**, (2005) 184410.
[14] C.P. Opeil, B. Mihaila, R.K. Schulze, L. Mañosa, A. Planes, W.L. Hults, R.A. Fisher, P.S. Riseborough, P.B. Littlewood, J.L. Smith, J.C. Lashley, Phys. Rev. Lett. **100** (2008) 165703.
[15] S.W. D'Souza, A. Rai, J. Nayak, M. Maniraj, R.S. Dhaka, S.R. Barman, D.L. Schlagel, T.A. Lograsso, A. Chakrabarti, Phys. Rev. B **85** (2012) 085123.
[16] S.W. D'Souza, R.S. Dhaka, A. Rai, M. Maniraj, J. Nayak, S. Singh, D.L. Schlagel, T.A. Lograsso, A. Chakrabarti, S.R. Barman, Mater. Sci. Forum **684** (2011) 215.
[17] A. Kimura, M. Ye, M. Taniguchi, E. Ikenaga, J.M. Barandiaran, and V.A. Chernenko, Appl. Phys. Lett. **103** (2013) 072403.
[18] A.N. Vasilev, A.D. Bozhko, V.V. Khovailo, I.E. Dikshtein, V.G. Shavrov, V.D. Buchelnikov, M. Matsumoto, S. Suzuki, T. Takagi, J. Tani, Phys. Rev. B **59** (1999) 1113.
[19] P.J. Webster, K.R.A. Ziebeck, S.L. Town, M.S. Peak, Philos. Mag. B **49** (1984) 295.
[20] R.S. Dhaka, S.W. D'Souza, M. Maniraj, A. Chakrabarti, D.L. Schlagel, T.A. Lograsso, S.R. Barman, Surf. Sci. **603**, (2009) 1999.
[21] P. Leicht, A. Laptev, M. Fonin, Y. Luo, K. Samwer, New J. Phys. **13**, (2011) 033021.
[22] P.J. Brown, J. Crangle, T. Kanomata, M. Matsumoto, K-U. Neumann, B. Ouladdiaf, K.R.A. Ziebeck, J. Phys. Condens. Matter **14** (2002) 10159.
[23] L. Righi, F. Albertini, G. Calestania, L. Pareti, A. Paoluzi, C. Ritter, P.A. Algarabel, L. Morellon, M.R. Ibarra, J. Solid State Chem. **179** (2006) 3525; L. Righi, F. Albertini, L. Pareti, A. Paoluzi, G. Calestani, Acta Mater. **55** (2007) 5237.
[24] S. Singh, J. Nayak, A. Rai, P. Rajput, A.H. Hill, S.R. Barman, D. Pandey, J. Phys. Condens. Matter **25** (2013) 212203.
[25] S. Singh, V. Petricek, P. Rajput, A.H. Hill, E. Suard, S.R. Barman, D. Pandey Phys. Rev. B **90**, (2014) 014109; S. Singh, J. Bednarcik, S.R. Barman, C. Felser, D. Pandey arXiv:1505.00119.
[26] S.W. D'Souza, J. Nayak, M. Maniraj, A. Rai, R.S. Dhaka, S.R. Barman, D.L. Schlagel, T.A. Lograsso, A. Chakrabarti, Surf. Sci. **606** (2012) 130.
[27] V.G. Sathe, A. Dubey, S. Banik, S.R. Barman, L. Olivi, J. Phys.: Condens. Matter **25** (2013) 046001; V.G. Sathe, S. Banik, A. Dubey, S.R. Barman, A.M. Awasthi, L. Olivi, Adv. Mater. Res. **52** (2008) 175.
[28] D.L. Schlagel, Y.L. Wu, W. Zhang, T.A. Lograsso, J. Alloy. Compd. **312** (2000) 77.
[29] S. Banik, A.K. Shukla, S.R. Barman, Rev. Sci. Instrum. **76** (2005) 066102; A.K. Shukla, S. Banik, S.R. Barman, Current Science **90** (2006) 490; M. Maniraj, S.R. Barman, Rev. Sci. Instrum. **85** (2014) 033301.
[30] R. Kundu, P. Mishra, B.R. Sekhar, M. Maniraj, S.R. Barman, Physica B **407** (2012) 827.
[31] S.K. Pandey, A. Kumar, S. Banik, A.K. Shukla, S.R. Barman, A.V. Pimpale, Phys. Rev. B **77** (2008) 113104; M. Maniraj, A. Rai, S.R. Barman, M. Krajčí, D.L. Schlagel, T.A. Lograsso, K. Horn, Phys. Rev. B **90** (2014) 115407; M. Maniraj, S.W. DSouza, S. Singh, C. Biswas, S. Majumdar, S.R. Barman, J. Elec. Spec. Rel. Phenom. **197** (2014) 106.
[32] S. Banik, A. Chakrabarti, U. Kumar, P.K. Mukhopadhyay, A.M. Awasthi, R. Ranjan, J. Schneider, B.L. Ahuja, S.R. Barman, Phys. Rev. B **74** (2006) 085110.
[33] H. Ebert et al., the Munich SPRKKR package, version 5.4, http://olymp.cup.uni-muenchen.de/ak/ebert/SPRKKR.
[34] S.W. D'Souza, T. Roy, S.R. Barman, A. Chakrabarti, J. Phys.: Condens. Matter **26** (2014) 506001.
[35] A. Fujimori, A. Minami, Phys. Rev. B **30** (1984) 957; S.R. Barman, D.D.

Sarma, Phys. Rev. B **51** (1995) 4007.
[36] R.S. Dhaka, S. Banik, A.K. Shukla, V. Vyas, A. Chakrabarti, S.R. Barman, B.L. Ahuja, B.K. Sharma, Phys. Rev. B **78** (2008) 073107.
[37] S.R. Barman, C. Biswas, K. Horn, Phys. Rev. B **69** (2004) 045413.